GOES NOP EUV Data, v2

Janet Machol, NOAA National Geophysical Data Center (NGDC) and University of Colorado, CIRES
Rodney Viereck, NOAA Space Weather Prediction Center (SWPC)
Andrew Jones, University of Colorado, LASP

22 May 2014

Table of Contents

1. Summary

The geostationary orbiting GOES 13-15 satellites were launched in 2006, 2009, and 2010 respectively. They each carry an Extreme Ultraviolet Sensor (EUVS) which measures the EUV in 5 bands (A-E) from about 5-127 nm as shown in Figure 1. The raw data is counts with a 10 s sample rate and a requirement of <15% uncertainty. NGDC currently provides calibrated data for the A, B and E bands for all three satellites. GOES 14 is unique in that it measures duplicate A and B bands (with the A' and B' channels) instead of C and D bands, and this data is available as well. Times of available GOES EUVS measurements are shown in Figure 2.

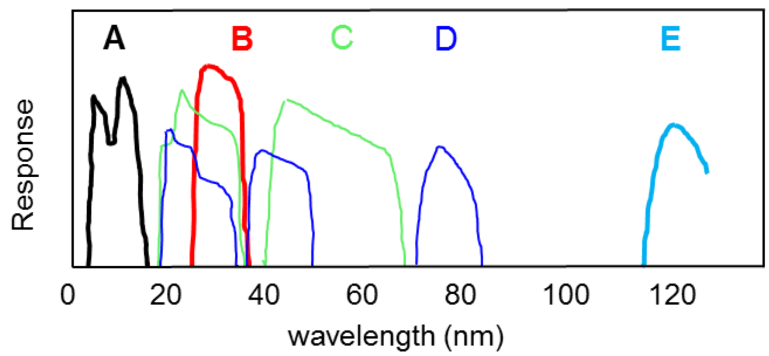

Figure 1. Wavelength responses of the GOES EUV sensors for the A-E bands.

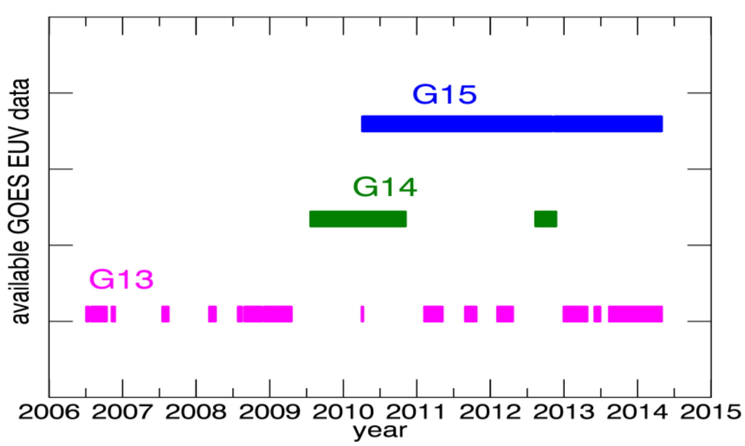

Figure 2. Available EUV measurements from GOES satellites. GOES 13 began operations in 2006, GOES 14 began in 2009, and GOES 15 began in 2010.

The raw count data is converted into irradiances using measured detector response curves and quiet sun reference spectra. In general, measurements of the A and B bands were found to agree well with other instruments and there was no noticeable degradation. The GOES-15 E channel has noticeable degradation which varies between instruments and did not seem to have the correct conversion factor -- the Lyman-α values were too high. Therefore we scaled the Channel E data by the SORCE SOLSTICE Lyman-α values with an exponential function that simultaneously corrects for degradation and the absolute value. The residual from this scaling is only a few per cent, and so this process provides corrected 1 minute Lyman-α data from GOES based on daily Lyman-α from SOLSTICE. Figure 3 through Figure 5 show the measured irradiances for the A, B, and E bands.

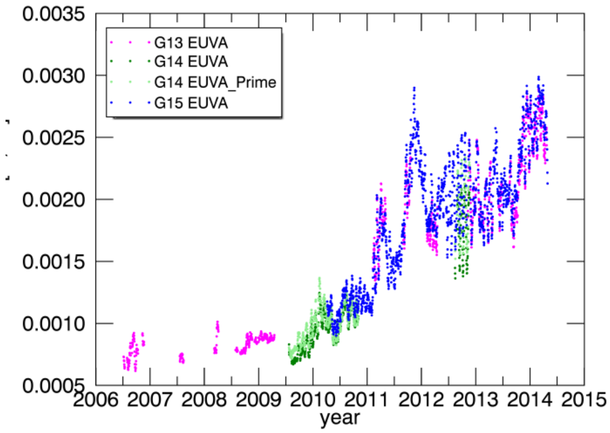

Figure 3. Irradiances for Channel A of GOES-13, -14 and -15. Irradiances for GOES-14 Channel A' are also shown.

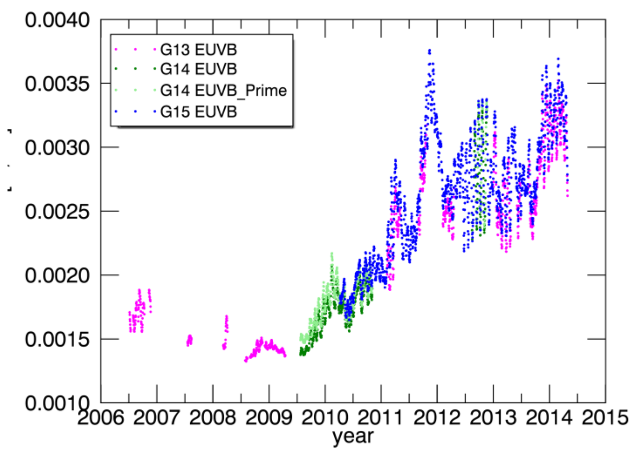

Figure 4. Irradiances for Channel B of GOES-13, -14 and -15. Irradiances for GOES-14 Channel B' are also shown.

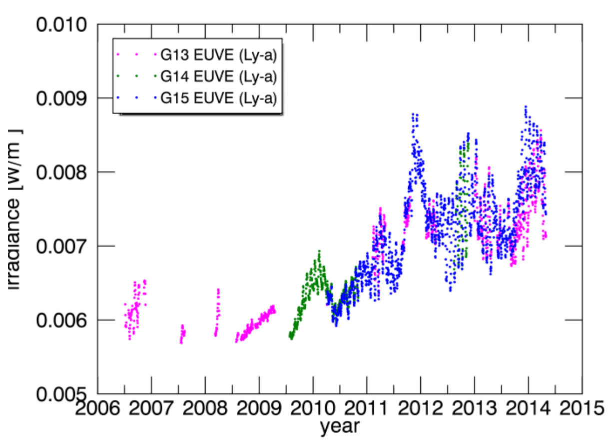

Figure 5. Irradiances from Channel E corrected to match the SORCE SOLSTICE Lyman-α band for GOES-13, -14 and -15.

The NGDC archive provides data files with 1-min and daily averaged counts and irradiances. The channel E files also contain 1-min and daily irradiances which have been adjusted to a 1-nm bandpass around the Lyman-α line and which are scaled to SORCE SOLSTICE with an exponential degradation. The data archive includes annual "quick look" plots. The data is currently available up to May 2014. The data processing is not yet automated, but the dataset will be updated periodically.

2. Data access

Annual files of counts and irradiances for for satellite (*nn*), channel (*c*), and year (*yyyy*) are at:

http://satdat.ngdc.noaa.gov/sem/goes/data/new_avg/*yyyy*/new_euv_temp/goes*nn*

G*nn*_EUV*c*_*yyyy*_v2.txt	1 minute data (counts and irradiances)
G*nn*_EUV*c*_*yyyy*_daily_v2.txt	daily data (irradiances
G*nn*_EUV*c*_irrad_ *yyyy*.png	plot of 1 minute and daily irradiances

Multi-year files are archived at:

http://satdat.ngdc.noaa.gov/sem/goes/data/new_avg/2014/new_euv_temp

.../multi_year/G*nn*_EUV*c*_y_{start}_y_{end}_daily_v2.txt	daily data for years y_{start} to y_{end}
.../AU_corr/AU_correction_factor_daily.txt	daily factor to convert data to 1AU, by doy
.../AU_corr/AU_correction_factor_daily_2006_2020.txt	daily factor to convert data to 1AU, by date

The files are ASCII and detailed column and format information is in the file headers. The daily files contain a 1 AU correction factor. To adjust the 1 min data to 1 AU, a user can interpolate the daily factors from either of the provided *AU_correction* files.

3. Data Calibration and Processing

The NOAA Space Weather Prediction Center (SWPC) gets raw count data with a cadence of 10.24 s from the GOES satellites. The counts are converted to calibrated fluxes with the equation:

$$\text{EUV Channel Irradiance } [\text{W/m}^2] = ((\text{Counts} - B\ [\text{counts}]) * G\ [\text{A/count}] - V\ [\text{A}]) / C\ [\text{A/(W/m}^2)] \quad \text{(Eq. 1)}$$

where for each channel, *B* is the background, *G* is the gain, *V* is the visible light contamination, and *C* is a units conversion factor. The values for the *G* and *V* come from the GOES-P Data and Calibration Handbook and are given in Table 3. The background values, *B*, are really electronic offsets, and are determined from the measurements when the satellite is pointed away from the Sun. The conversion factors are determined based on the measured detector spectral responses convolved with a quiet sun spectrum and change with solar activity level (Table 4). Response curves for the channels A, B and E for GOES-15 are shown in Figure 6 through Figure 10 along with reference spectra for a quiet sun during solar minimum and maximum. Reference spectra from the Naval Research Laboratory are used to define the calibration factors for EUVS-A and -B and the LASP WHI quiet period spectrum was used for EUVS-E. The responses for the different satellites are similar but not identical.

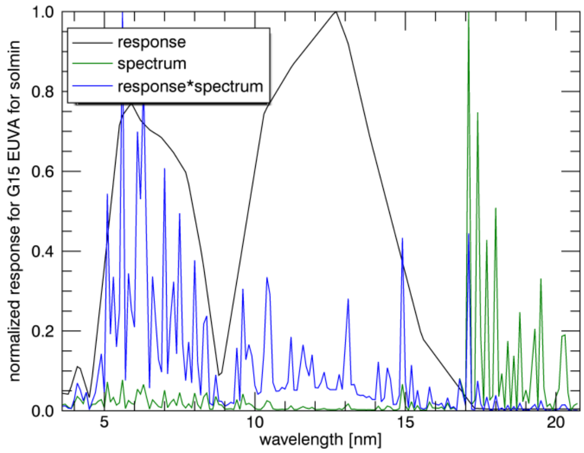

Figure 6. Response curve, solar minimum spectrum and response*spectrum for Channel A on GOES 15.

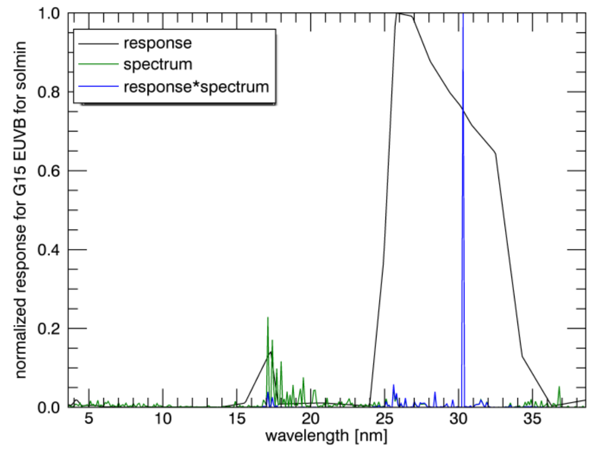

Figure 8. Same but for solar minimum for Channel B.

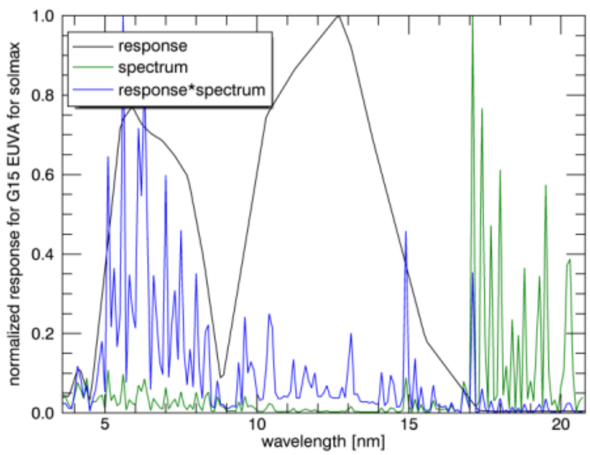

Figure 7. Same but for solar maximum for Channel A.

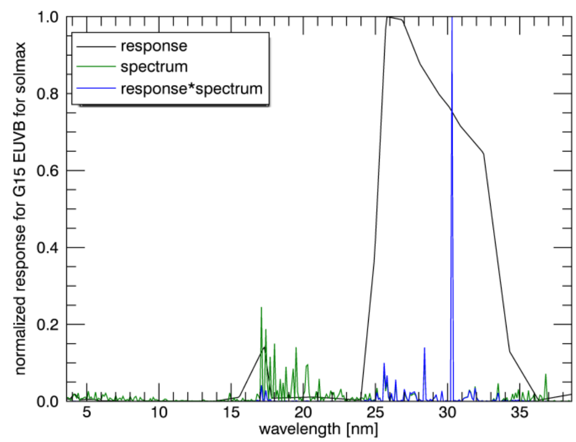

Figure 9. Same but for solar maximum for Channel B.

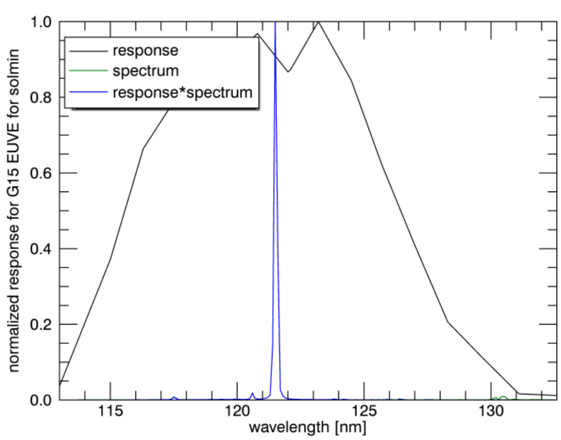

Figure 10. Same but for solar minimum for Channel E.

We removed spikes and dropouts before combining the count data into 1 minute averages. The A channel counts are also cleaned of spikes from noise from the Solar X-ray Imager (SXI) heater as described in Appendix B2. Starting around 2010, the 10 s count data provides flags for bad/missing data, off-pointing, calibrations and eclipses. The one minute averages use the flags given in Table 1. We also set a 'partial eclipse flag' for times near eclipses to show that the count values are reduced by thermal effects. The daily data is an average of all 1 min data with flags of 0 or 1, and uses only three flags, 0 and 1 for good data and -999 for bad data. The 1 min and daily files have time stamps in the center of the period. More details of how the flags are set are given in Appendices B1 and B5.

Table 1. Flags and values in averaged data. Actual counts or irradiance values are denoted as *x*.

flag	definition	flags in 10-s source records	counts	irradiance
0	no flag	all data in average had flag=0 and no partial eclipse	*x*	*x*
1	possible bad data	Used in GOES14 Chan E before 1 December 2010 when there appears to be a different degradation rate based on fit to SOLSTICE Lyman-α data; included in daily values	*x*	*x*
2	partial eclipse	Flag set to 0 in 1-minute average routine. Later analysis adds partial eclipse flags near times with eclipses.	*x*	*x*
5	eclipse	At least one eclipse flag (flag >4,000,000) and no off-point or calibration flags.	-999	-999.0
8	off-pointed or in-flight calibrations	At least one off-point or calibration flag (1,000,000 < flag < 4,000,000)	-999	-999.0
-999	bad or missing data	all flags were -99999	-999	-999.0

An example of a comparison of 1 min and daily irradiance values is shown in Figure 11. Plots like these are available in the archive. The Channel E plots include lines to show the corrected Lyman-α subband and the impact of the 1-AU correction. Low points are due to imperfect removal of eclipse, offpoint, and calibration data. Eclipse seasons are centered about April and October.

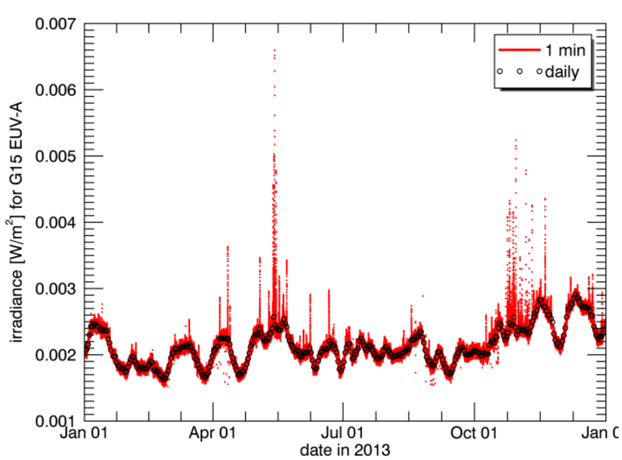

Figure 11. Irradiance plot with 1 min and daily averages for 2013 for GOES-15 Channel A.

Channel E data is converted to a 1 nm band around the Lyman-α line at 121.6 nm by scaling based on the LASP WHI quiet sun reference spectrum. The scaling factor is about 88% (Table 4 in Appendix A). The E channel suffers degradation, and so to remove the degradation, the data is scaled to SORCE SOLSTICE Lyman-α measurements. The ratio of the daily averaged GOES Lyman-α to the daily SOLSTICE Lyman-α is fit with an exponential, $y(t)=a \exp[b(t- t_0)] + c$ for time, t. The daily and one minute GOES Lyman-α data is then divided by this function which scales the data to SOLSTICE and corrects for degradation. The amount of degradation for Channel E as a function of year is given in Table 2. The factors for the exponential scaling function are given in Table 9 in Appendix A.

Table 2. Amount of degradation for Channel E after a given number of years based on the fit parameters in Table 9.

	after: 1 year	2 years	5 years
GOES13	3%	5%	10%
GOES14	6%	7%	7%
GOES15	13%	22%	35%

4. Comparisons with other satellite data sets

This section shows time series of GOES irradiances as well as comparisons with the following calibrated data sets: SDO EVE, version 4; SOHO SEM, version 3; and SORCE SOLSTICE Lyman-α, version 12. To compare the irradiance for the GOES Channels A and B with irradiance from another satellite instrument we estimated the fraction of the GOES channel irradiance that would fall in the other instrument bandpass as described in Appendix B4. The GOES data was adjusted to 1 AU for the comparisons with the other data sets. The SOHO SEM data has 17-nm scatter into this band which sometimes results in a double-humped peak for each solar rotation since it is has an angular factor (A. Jones, personal communication). Major sources of discrepancies between data sets are calibration errors, incomplete correction for differing bandpasses, and the use in the GOES calibrations of solar minimum reference factors instead of factors that vary with solar activity.

4.1 GOES-15

4.1.1 GOES 15 Channel A

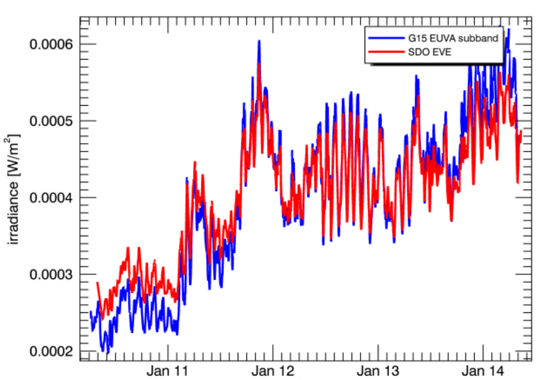

Figure 12. Comparison of the EVE GOES-A band (derived from MEGS A for the 5 to 15 nm band) with a subset of the GOES-15 Channel A data from 5-15 nm.

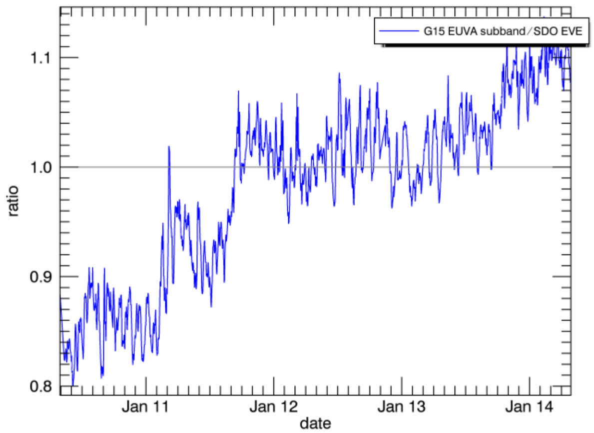

Figure 13. Ratio of GOES-15 EUV-A to EVE GOES-A band.

4.1.2 GOES-15 Channel B

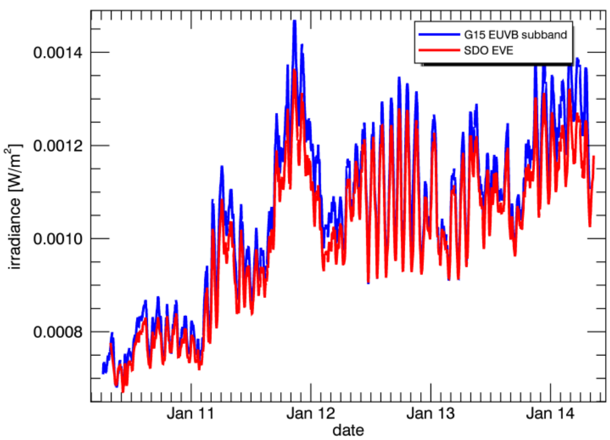

Figure 14. Comparison of the EVE GOES-B band with subset of the GOES-15 Channel B data from 25-34 nm.

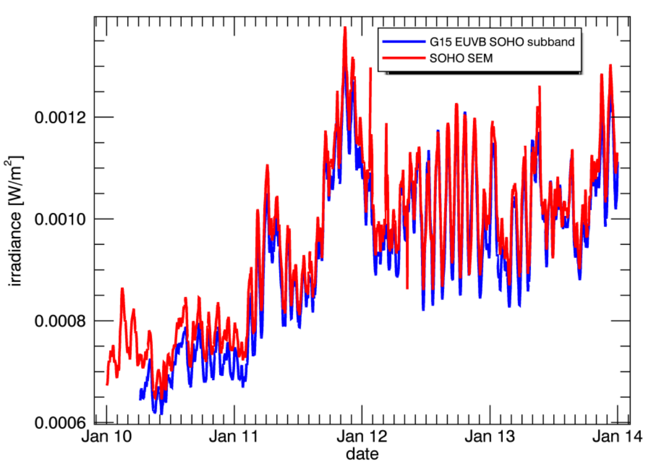

Figure 15. Comparison of the SOHO SEM 26-34 nm band with subset of the GOES-15 Channel B data from 26-34 nm.

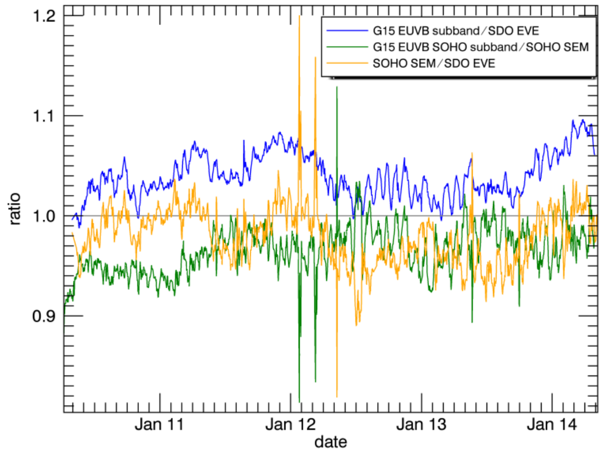

Figure 16. Ratios between GOES 15 EUVS-B, SDO EVE, and SOHO SEM.

4.1.3 GOES-15 Channel E

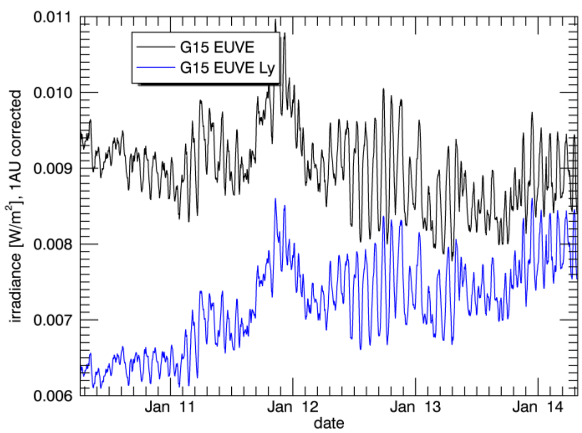

Figure 17. The GOES-15 EUVS-E data and the 1 nm Lyman-α subband (121.0 -121.9 nm) before degradation correction.

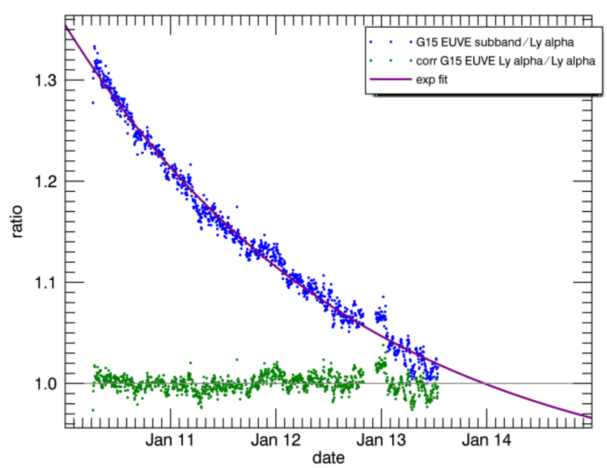

Figure 18. Ratio of GOES-15 EUVS-E to the SOLSTICE elements of the SORCE SOLSTICE Lyman-α (blue dots). The ratio is fit (purple line) with the function $y=a\bullet\exp[b(t-t_0)] + c$. This fit is used both to determine the decay rate and to correct the data. The anomalous period from 1 Dec 2012 to 20 Jan 2013 was excluded for the fit generation. The residual (green dots) is <±3%.

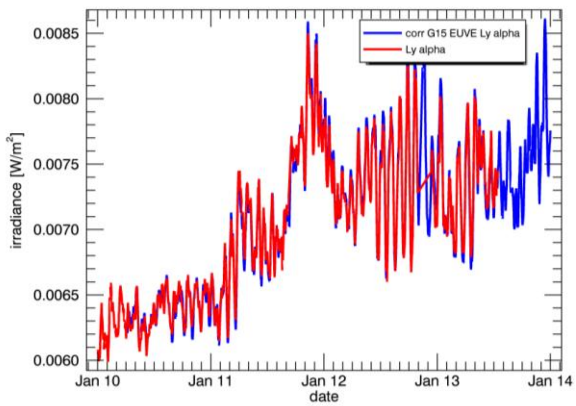

Figure 19. Comparison of the scaled and degradation-corrected GOES-15 Channel E data from 121.0-121.0 nm to the SORCE SOLSTICE Lyman-α.

4.2 GOES-14

4.2.1 GOES-14 Channels A and A'

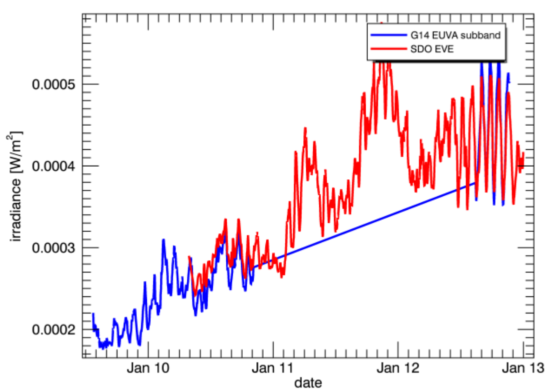

Figure 20. Comparison of the EVE GOES-A band (derived from MEGS A for the 5 to 15 nm band) with a subset of the GOES-14 Channel A data from 5-15 nm.

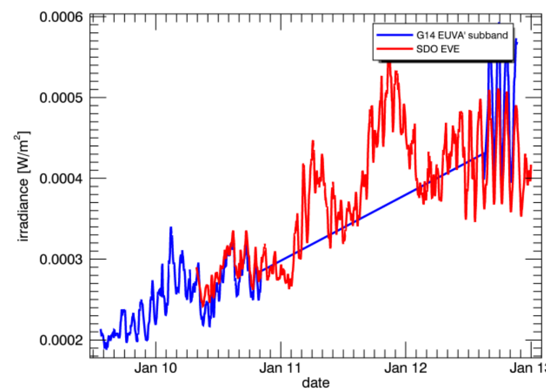

Figure 21. Comparison of the EVE GOES-A band (derived from MEGS A for the 5 to 15 nm band) with a subset of the GOES-14 Channel A' data from 5-15 nm.

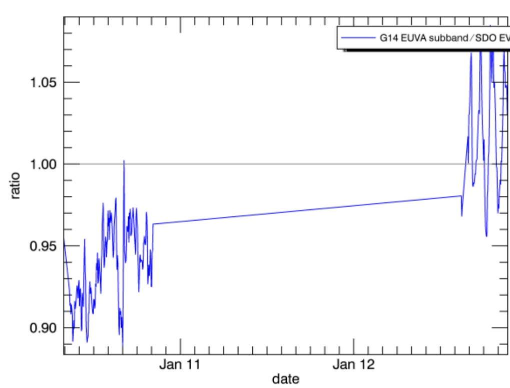

Figure 22. Ratio of GOES-15 EUV-A to EVE GOES-A band.

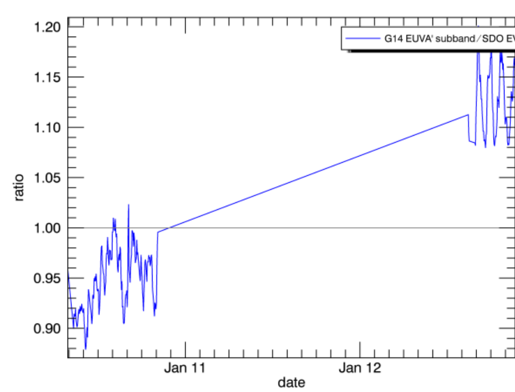

Figure 23. Ratio of GOES-15 EUV-A' to EVE GOES-A band.

4.2.2 GOES-14 Channels B and B'

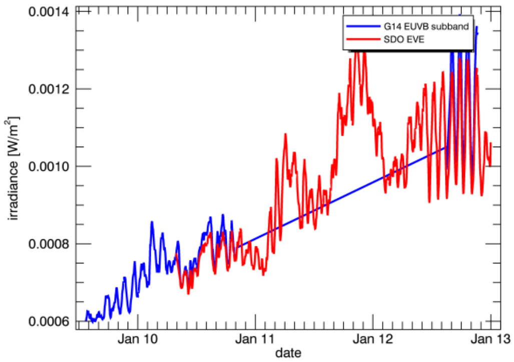

Figure 24. Comparison of the EVE GOES-B band with subset of the GOES-14 Channel B data from 25-34 nm.

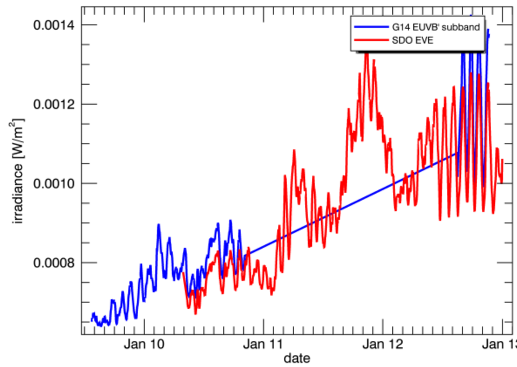

Figure 25. Comparison of the EVE GOES-B band with subset of the GOES-14 Channel B' data from 25-34 nm.

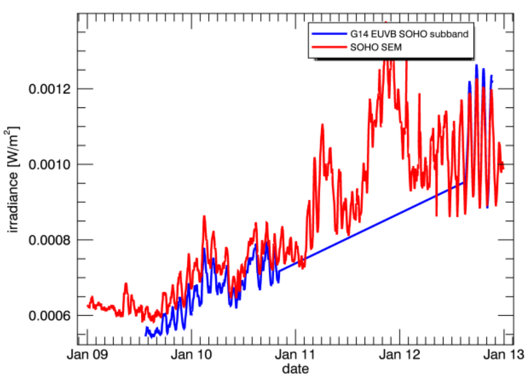

Figure 26. Comparison of the SOHO SEM 26-34 nm band with subset of the GOES-14 Channel B data from 26-34 nm.

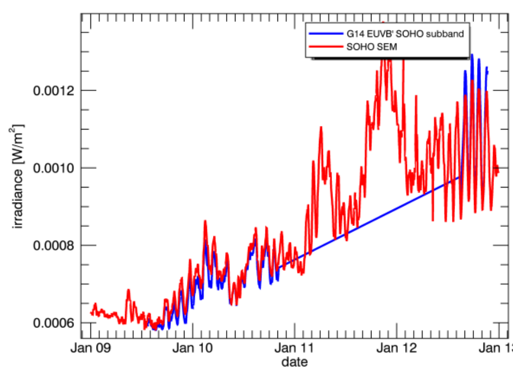

Figure 27. Comparison of the SOHO SEM 26-34 nm band with subset of the GOES-14 Channel B' data from 26-34 nm.

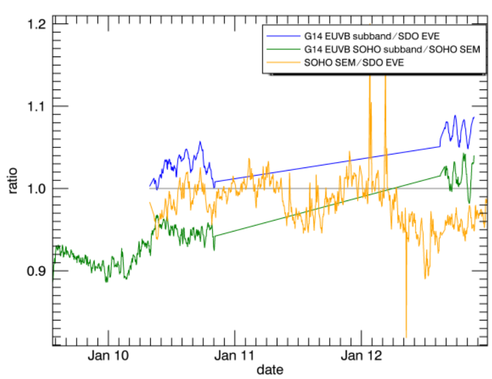

Figure 28. Ratios between GOES 14 EUVS-B, SDO EVE, and SOHO SEM.

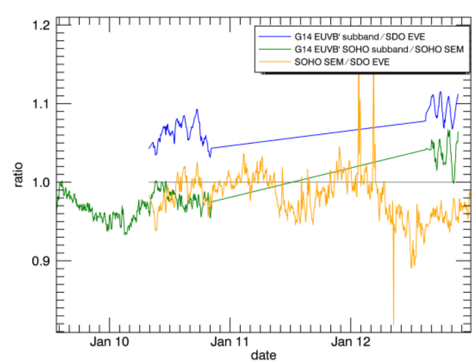

Figure 29. Ratios between GOES 14 EUVS-B', SDO EVE, and SOHO SEM.

4.2.3 GOES-14 Channel E

The GOES-14 Channel E data was fit starting 1 Dec 2009. The Channel E measurements prior to this date appears to have a much slow decay and the reason for this is not known. It is recommended that the data prior to 1 Dec 2009 not be used the flags for this time period have been set to 1 to note that it has a questionable calibration.

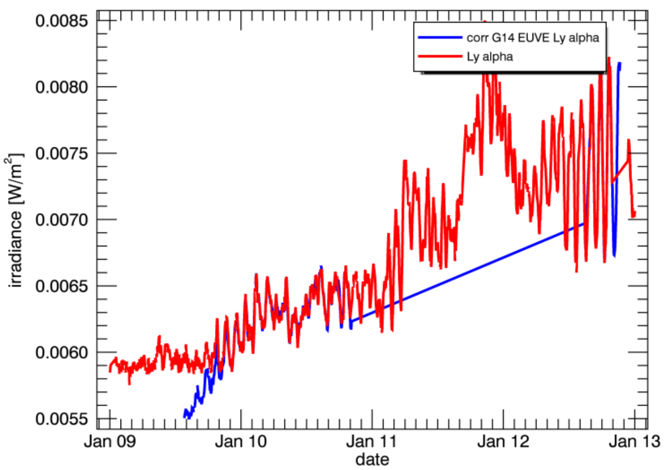

Figure 30. Comparison of the scaled and degradation-corrected GOES-14 Channel E data from 121.0-121.0 nm to the SORCE SOLSTICE Lyman-α.

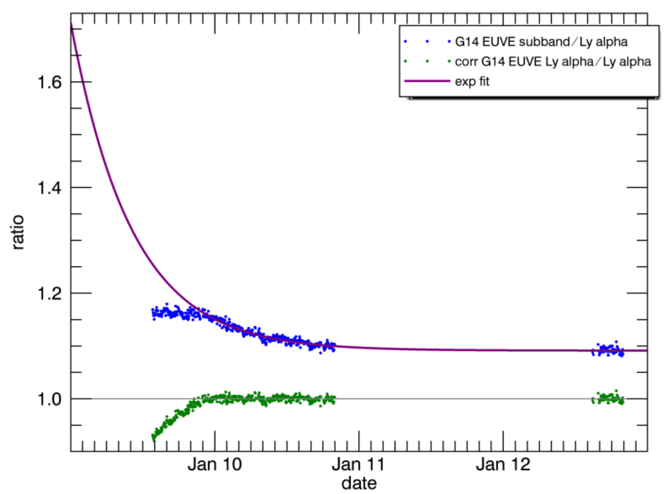

Figure 31. Ratio of GOES-14 EUVS-E to the SOLSTICE elements of the SORCE SOLSTICE Lyman-α (blue dots). The ratio is fit (purple line) with the function y=a•exp[b(t-t0)] + c for the period after 1 Dec 2009. The green dots show the residual which is very low after 1 Dec 2009.

4.3 GOES-13

4.3.1 GOES-13 Channel A

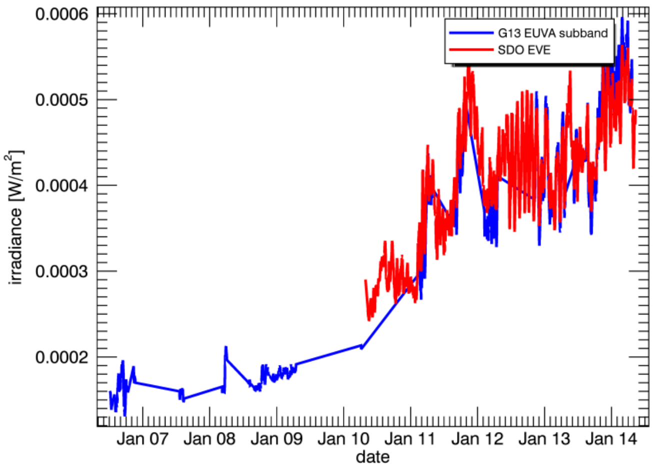

Figure 32. Comparison of the EVE GOES-A band (derived from MEGS A for the 5 to 15 nm band) with a subset of the GOES-13 Channel A data from 5-15 nm.

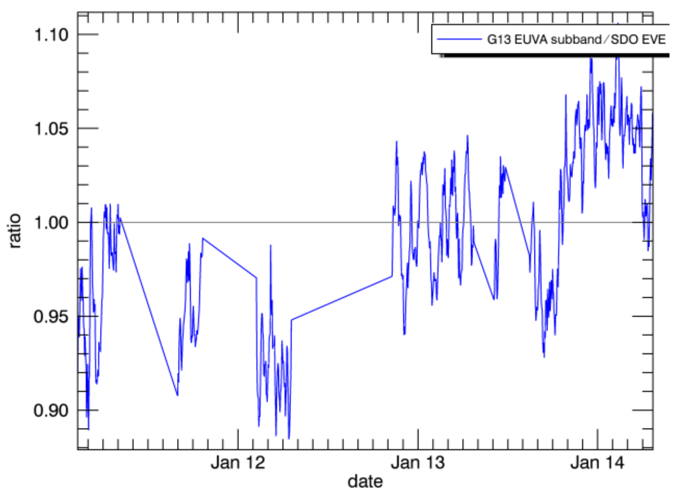

Figure 33. Ratio of GOES-13 EUV-A to EVE GOES-A band.

4.3.2 GOES-13 Channel B

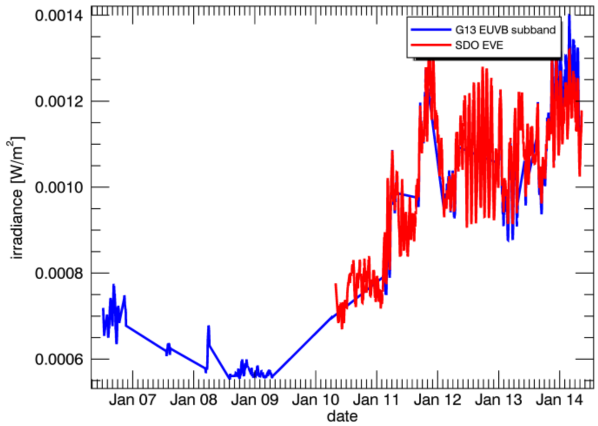

Figure 34. Comparison of the EVE GOES-B band with subset of the GOES-13 Channel B data from 25-34 nm.

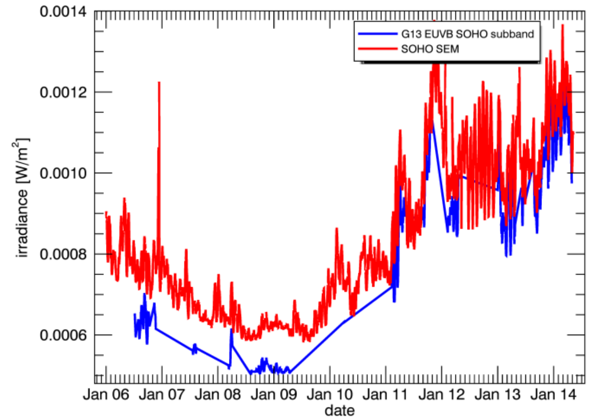

Figure 35. Comparison of the SOHO SEM 26-34 nm band with subset of the GOES-13 Channel B data from 26-34 nm.

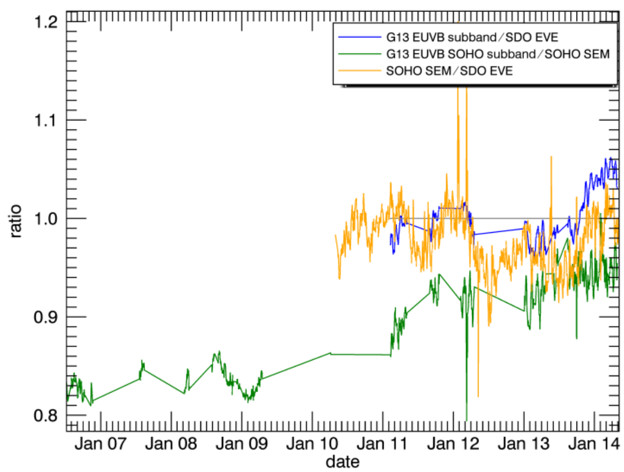

Figure 36. Ratios between GOES 13 EUVS-B, SDO EVE, and SOHO SEM.

4.3.3 GOES-13 Channel E

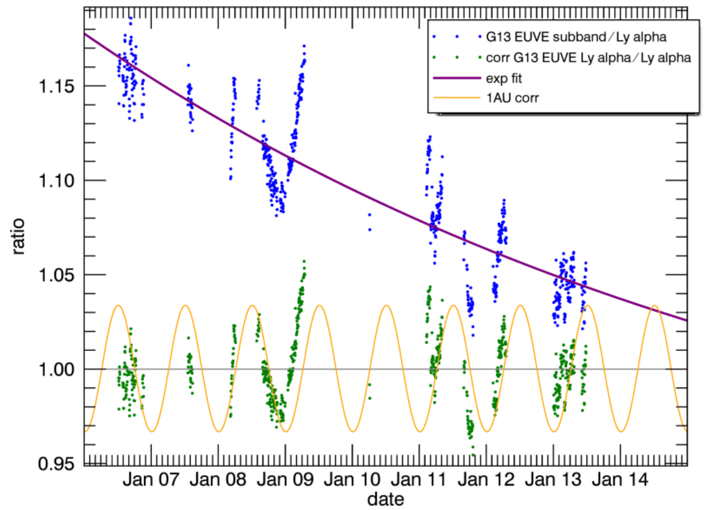

Figure 37. Ratio of GOES-13 EUVS-E to the SOLSTICE elements of the LASP Lyman-α Composite (blue dots). The ratio is fit (purple line) with the function y=a•exp[b(t-t0)] + c. The 1AU correction is shown as a guide to the eye for possible future seasonal temperature corrections.

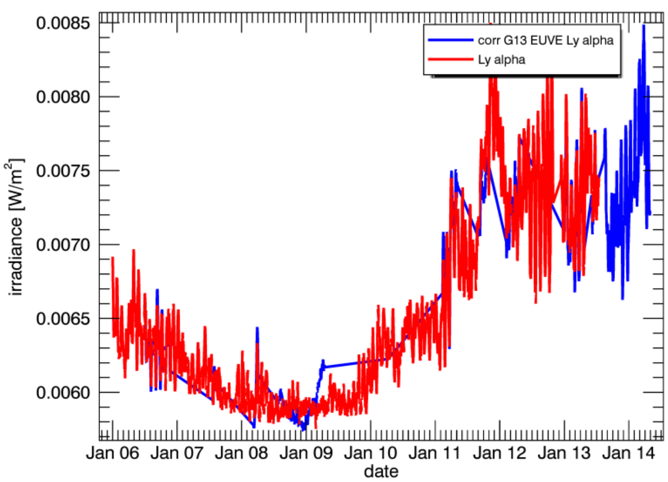

Figure 38. Comparison of the scaled and degradation-corrected GOES-13 Channel E data from 121.0-121.0 nm to the SORCE SOLSTICE Lyman-α.

5. Future improvements to the data

There are number of refinements that can be done on the EUVS data processing. These include:

- Automate file creation.
- Consider using other reference spectra.
- Determine how best to apply reference spectra that vary with solar activity.
- Create flags for years prior to 2010.
- Exclude dips due to the geocoronal absorption in the Channel E daily irradiances. The impacts are biggest at the equinoxes. The dips are roughly 6% and last 3 hours per day around the equinoxes. For daily averaging, this results in about a 1% change. Flag these data in the 1 minute averages.
- Derive uncertainties on the data including uncertainties due to detector response functions.
- Determine best way to combine duplicate A and B channels on GOES 14 to get cleaner data.
- Process Channels C and D on GOES 13 and 15.
- Consider creating composites with data from all three satellites.
- Automate file creation

References

Viereck, R., F. Hanser, J. Wise, S. Guha, A. Jones, D. McMullin, S. Plunket, D. Strickland, S. Evans (2007), "Solar extreme ultraviolet irradiance observations from GOES: design characteristics and initial performance", Proc. SPIE 6689, Solar Physics and Space Weather Instrumentation II, 66890K, doi:10.1117/12.734886.

Contacts

Comments and questions regarding the archived GOES EUVS data may be sent to janet.machol@noaa.gov.

Appendix A. Calibration Tables

The values in the tables in Appendices A1, A2, and A3 are used with Eq. 1 to convert count rates into irradiances. The scale factors in the tables are used to scale the bandpasses of the GOES channels to match the bandpasses of other instruments. Table 9 provides the fit parameters to correct for degradation in the Channel E Lyman-α data for all three satellites.

A1. Tables for GOES 13

Table 3. Correction factors for GOES 13. Gain and background values are for a telescope temperature of 12C. Background is used as an offset.

channel	Background [counts]	Gain [A/counts]	Visible Light Contamination [A]	bandpass [nm]
A	25198	1.91E-15	2.13E-14	2.8-20.6
B	15970	1.89E-15	1.21E-14	2.8-36.4
C	16229	1.90E-15	4.79E-14	-
D	24387	1.89E-15	1.20E-15	-
E	25096	1.90E-15	1.32E-12	113.5-132.8

Table 4. Flux conversion factors, *C*, for GOES-13 channels for solar minimum and maximum conditions. Also shown are scale factors, *f*, to match the bandpasses of other instruments.

channel	solar activity	C[A/(W/m^2)]	f_{EVE} 5-15 nm	f_{EVE} 25-34 nm	f_{SOHO} 26-34 nm	$f_{Lyman-\alpha}$ 121.0-121.9 nm
A	minimum	8.918e-10	0.21	-	-	-
A	maximum	8.065e-10	0.19	-	-	-
B	minimum	6.615e-09	-	0.406	0.368	-
B	maximum	6.034e-09	-	0.381	0.335	-
E	minimum	2.612E-09	-	-	-	0.884

A2. Tables for GOES 14

Table 5. Correction factors for GOES 14. Gain and background values are for a telescope temperature of 12C. Background is used as an offset.

channel	Background [counts]	Gain [A/counts]	Visible Light Contamination [A]	bandpass [nm]
A	26571	1.92E-15	1.04E-14	2.8-19.0
B(A')	23948	1.93E-15	7.18E-14	2.8-19.0
C (B)	14207	1.93E-15	2.96E-13	6.0-36.6
D (B')	24856	1.95E-15	5.47E-14	6.0-36.6
E	25188	1.94E-15	2.49E-12	113.7-135.9

Table 6. Flux conversion factors, *C*, for GOES-14 channels for solar minimum and maximum conditions. Also shown are scale factors, *f*, to match the bandpasses of other instruments.

channel	solar activity	C[A/(W/m^2]	f_{EVE} 5-15 nm	f_{EVE} 25-34 nm	f_{SOHO} 26-34 nm	$f_{Lyman\text{-}\alpha}$ 121.0-121.9 nm
A	minimum	8.718e-10	0.256	-	-	-
A	maximum	8.691e-10	0.248	-	-	-
A'	minimum	8.744e-10	0.256	-	-	-
A'	maximum	8.628e-10	0.248	-	-	-
B	minimum	4.841e-09	-	0.424	0.385	-
B	maximum	4.441e-09	-	0.406	0.357	-
E	minimum	2.630e-09	-	-	-	0.855

A3. Tables for GOES 15

Table 7. Correction factors for GOES 15. Gain and background values are for a telescope temperature of 12C. Background is used as an offset.

channel	Background [counts]	Gain [A/counts]	Visible Light Contamination [A]	bandpass [nm]
A	49454	1.91E-15	1.78E-14	3.6-20.8
B	49797	1.90E-15	2.71E-14	3.6-38.5
C	55451	1.90E-15	2.03E-15	-
D	51218	1.90E-15	4.37E-14	-
E	40947	1.90E-15	2.23E-12	116.3-132.4

Table 8. Flux conversion factors, *C*, for GOES-15 channels for solar minimum and maximum conditions. Also shown are scale factors, *f*, to match the bandpasses of other instruments.

channel	solar activity	C[A/(W/m^2]	f_{EVE} 5-15 nm	f_{EVE} 25-34 nm	f_{SOHO} 26-34 nm	$f_{Lyman\text{-}\alpha}$ 121.0-121.9 nm
A	minimum	1.100e-09	0.213	-	-	-
A	maximum	1.006e-09	0.193	-	-	-
B	minimum	3.786e-09	-	0.399	0.363	-
B	maximum	3.594e-09	-	0.379	0.333	-
E	minimum	2.348e-09	-	-	-	0.884

A4. Lyman-α fit parameters

Table 9. Fit parameters for the to the function $y(t)=a \exp[b(t- t_0)] + c$ for time, *t*, in units of Julian Day. The Lyman-α data from Channel E is corrected for degradation and scaled to SOLSTICE by dividing by this function. The fit for GOES14 starts on 1 Dec 2009.

	a	b	c	t_0 [Julian Day]
GOES13	0.22656203	-0.00032264091	0.92886897	2454302
GOES14	0.071629217	-0.0064360812	1.0913027	2455168
GOES15	0.42309890	-0.00098659526	0.88899175	2455294

Appendix B. Processing Procedure

B1. Count averages and flags

The raw data is 10-s count data from SWPC which has time stamps at the beginning of the time periods. The data is first cleaned by removing points with anomalously high or low counts. Each 10-s record with good data is averaged into the minute period in which its midpoint lies. The raw data exact spacing is 10.24 s, and so 97% of the 1-min averages contain 5 or 6 raw records. About 3% of the 1-min records have no data (flags 5, 8 or 9). Starting in 2010, the raw data provided from SWPC has the flags listed in Table 10. The 10-s flags are combined to create flags for the minute data files as described in Table 1.

A partial eclipse flag is set in the one minute data records adjacent to ones flagged for eclipses. The number of minutes of partial eclipse flag on either side of an eclipse depends on the duration of the eclipse and these numbers were found empirically. Partial eclipse flags are set for 8 mins before and 5 mins after eclipse periods longer than 30 mins, and for 12 mins before and 10 mins after eclipse periods shorter than 30 mins.

Table 10. Flags in 10-s count data. Real count values are denoted as *x*.

flag	definition	counts
0	no flag	*x*
-99999	bad or missing data	-99999
1048576	in-flight calibration	*x*
2097152	off-pointed	*x*
3145728	off-pointed and in-flight calibrations	*x*
4194304	Sun is eclipsed by the Moon	*x*
8388608	Sun is eclipsed by the Earth	*x*
12582912	Sun is eclipsed by the Moon and the Earth	*x*
14680064	Sun has unknown eclipsed (Moon or Earth)	*x*

B2. Channel A temperature correction

The GOES NOP EUV-A Channel data has noise spikes that are correlated with the Imager Mounting Platform (IMP) heater. The heater is required to keep the IMP at a stable temperature. It has fixed set points that are not controllable from the ground. During the coldest parts of the GOES season (summer), the heaters cycle about every 10 – 50 minutes. During the warmest parts of the GOES season (winter) the heaters are sometimes not required at all and may stay off for weeks at a time.

A temperature gradient across two dissimilar metal components of the IMP may be producing very small currents that get into the EUV-A detector signal current. Thus, as the IMP is warmed by the heater, a reverse current combined with the EUV-A detector current makes the net signal go down. When the heater goes off, the plates cool, and the current goes the other way, thus increasing the signal from the detector. Only the EUV optical housing that is mounted closest to the IMP seems to experience this heater noise. And within that housing, only the A channel seems noticeably affected. In some of the

EUVS sensors, the heater noise can be seen in the B channel (mounted in the same optical housing) but this noise is vastly reduced and is therefore not removed from the signal.

The heater noise is partially removed from the GOES EUV-A data by using the SXI PCM2 temperature sensor as a proxy for the heater with a routine developed by R. Viereck. The SXI PCM2 temperatures are sampled about every 30 s. To process these data, first the noise spikes and outliers are removed from the count data and then a 7 point or 3.5 minute box-car smoothing is applied. The first derivative of the temperature is then calculated. This first derivative looks very similar to the heater noise in the EUV-A signal. The derivative of the SXI PCM2 temperature is scaled to fit the EUV-A signal. A small time shift of the SXI PCM2 data is required to maximize the fit of the SXI PCM2 data to the EUV-A data but this shift and the scaling remain constant throughout the mission. An example of the Channel A data with the heater noise and the heater noise correction is shown in Figure 39.

The smoothing and the time-shifting of the SXI PCM2 data make it impossible to calculate the correction in real-time; however, the delay introduced by this process is less than 5 minutes. For GOES-15, the impact of the heater noise has not changed since launch. Heater noise corrections were done for GOES 13 and 15 only, because on GOES-14, there is SXI heater data only for 2009. On GOES 14, the A channel is expected to be much more impacted than the A' channel.

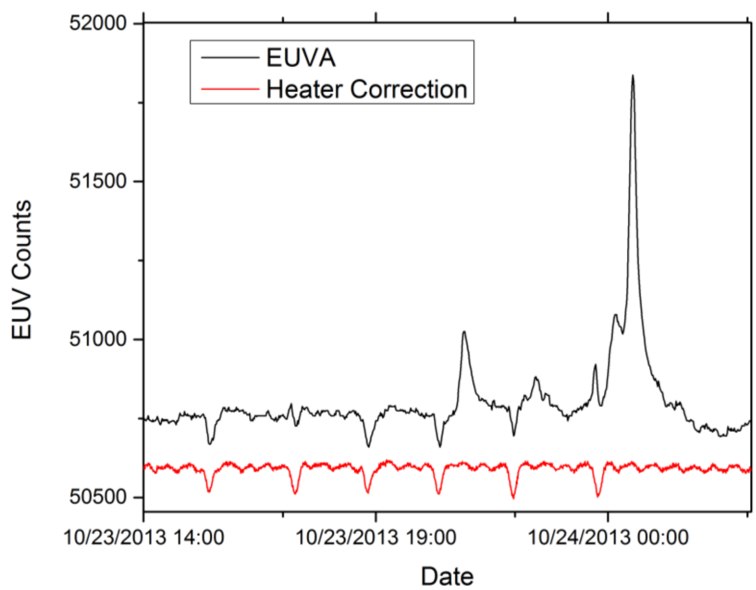

Figure 39. Channel A counts (black) showing heater noise and correction (red) based on SXI heater current.

B3. Calibrations

The original calibrations in the Handbook were done by ATC with the EUV beam at Brookhaven National Laboratory. The background values, *B*, do not vary much in time after the initial few months. We rederived these values by looking at measurements during satellite off-points. We also rederived the conversion values, *C*, since the ones in the Handbook are of poor quality; they were created with a flat spectrum and are given in the wrong units --- [A/(W/m^2-nm] instead of [A/(W/m^2]. Previously, also, SWPC applied empirical correction factors in the conversion from counts to fluxes for each satellite and channel; these are no longer used.

The NRL spectrum was used for Channels A and B, while the LASP WHI spectrum was used for Channel E. After applying a 1AU correction to the data, it was compared with daily values from other instruments to test the calibrations. SDO EVE data was used for Channel A comparisons, SDO EVE and SOHO SEM data were used for Channel B, and SORCE SOLSTICE Lyman-α was used for Channel E comparisons.

B4. Calibrations with the model spectra

Currently we do calibrations with the quiet sun spectra. For the shorter wavelengths (channels A-D) we use the NRLEUV 2 updated Model Quiet Sun Irradiance Spectrum, while for the Channel E around Lyman-α we use the LASP WHI quiet sun spectrum.

The photon irradiance values are given per 0.5 nm. Let's convert these to W m^{-2}. The resolution of 0.5 nm does not impact the equations; it is carried through.

The photon irradiance J_i are in units of [$\gamma\ cm^{-2}\ s^{-1}\ (0.5\ nm)^{-1}$]
The desired units are J_i[W m^{-2} $(0.5\ nm)^{-1}$].

E/photon= $hc/\lambda[m]\ \gamma^{-1} = hc/(\lambda[nm] \cdot 10^{-9}[m/nm])\ \gamma^{-1}$
with h=6.626x10^{-27} erg ·s, $c = 3 \times 10^8\ m\ s^{-1}$, and 1 W= 10^7 erg s^{-1}

The conversion is then

$$J_i[W\ m^{-2}\ (0.5\ nm)^{-1}] = J_i[\gamma\ cm^{-2}\ s^{-1}\ (0.5\ nm)^{-1}] \cdot hc/(\lambda[nm] \cdot 10^{-9}[m/nm])\ \gamma^{-1}$$

$$= \frac{J_i[\gamma\ cm^{-2}\ s^{-1}\ (0.5\ nm)^{-1}]\ \gamma^{-1} \cdot 10^{9}\ [nm\ m^{-1}] \cdot (6.626\times10^{-27}\ erg \cdot s \cdot 3\times10^{8}\ m\ s^{-1})\ (1W \cdot 10^{-7}\ erg^{-1}\ s) \cdot [10^{4}\ cm^{2} \cdot m^{-2}]}{\lambda[nm]}$$

$$= \frac{J_i[cm^{-2}\ s^{-1}\ (0.5\ nm)^{-1}] \cdot 1.988\times10^{-12}\ [(cm^{2}\ s\ nm)\ (W\ m^{-2})]}{\lambda[nm]}$$

For the quiet regime, the total irradiance over the band is given by

$$J_{tot\_quiet}\ [W\ m^{-2}] = \sum_i J_i[\mathrm{W\ m^{-2}\ (0.5\ nm)^{-1}}]$$

The current for the quiet time is given by

$$I_{tot\_quiet}[A] = \sum_i\ R_i[A\ m^2\ W^{-1}] \cdot J_i[\mathrm{W}\ m^2\ (0.5\ \mathrm{nm})^{-1}]$$

So now, if we measure a current, I_{meas}, during a quiet time, then the total flux in the band is

$J_{tot\_meas} = (J_{tot\_quiet} / I_{tot\_quiet}) \cdot I_{meas}$

To compare with another instrument on a different type of satellite, we scale the total flux by the fraction of the flux that is in the bandpass of the other instrument. We can also estimate the fraction of irradiance in energy units in some band subset with

$$f_{subset} = \sum_i J_i[\mathrm{W\ m^{-2}\ (0.5\ nm)^{-1}}] \ / \ J_{tot\_quiet}\ [W\ m^{-2}] \quad \text{where } i \text{ is in subset}$$

More details such as impacts of solar activity, angle, particle backgrounds and limb effects could be considered. As a next step, comparison should be done for regimes based on solar activity, at least a quiet regime and a flare regime.

Assuming solar maximum instead of solar minimum conditions can result in a 10% increase in the irradiance. However, when the bandpasses are scaled to match other instruments, sometimes the variability in f sometimes almost exactly cancels the variability in C, and so the net ratio between the instrument measurements does not change significantly.

Appendix C. GOES EUVS hardware

The EUVS on GOES-13-15 were all very similar. The five channels of the EUV were measured via three spectrograph units with east-west dispersion. The units vary in the grating spacing, For GOES 13 and 15, the first unit measure channels A and B and the second unit measures channel s C and D. For GOES 14, the first unit measures channels A and B, and the second unit measures channels A' and B'. The measurements are redundant except that the A'-B' detectors are arranged in opposite order so that they have opposite impacts of angular effects from sources near the solar limb. The intent is that each pair of channels can be averaged to produce an irradiance with reduced error due to angular effects. For all three GOES satellites, Channel E is measured on a separate spectrograph. Sample rates are once every 32.768 s. Table 11 shows some details of the spectrograph elements, specifically the hardware design, manufacturer, components, contamination and degradation.

Table 11. Hardware components for EUVS on GOES 13-15. Note that on GOES-14, the C and D channels are at the usual A and B wavelengths.

instrument/component	manufacturer	details
EUVS	ATC	There are 3 optical benches: one for A and B, one for C and D (or A' and B' on GOES-14), and one for E. Nominal wavelengths (nm) are: A: 5-15, B: 25-34, C: 17-67, D: 17-84, E: 118-127
detectors	IRD	AXUV photodiode On GOES-14,channels B, B' and E are nitrided.
gratings	MIT	A,B: 5000 lines/mm C,D: 2500 lines/mm E: 1667 lines/mm
thin film filters on detectors	Lebow	A: 50/200/70 nm of Ti/Mo/C B: 150/5 nm of Al/Al_2O_3 C: 150/2 nm of Al/Al_2O_3 D: 150/2 nm of Al/Al_2O_3

Lyman-α filter	Acton Labs	free standing

According to Viereck et al. (2007), several design features and manufacturing techniques were incorporated to minimize the impact of contamination. The first optical component is the transmission grating. The buildup of contaminants from outside the sensor will occur primarily on the grating bars which will have minimal impact on the transmission properties. The grating can accumulate 10's of nm of molecular contaminants before experiencing a noticeable change in transmission whereas an optical component such as a filter or window will exhibit a significant decrease in performance (depending on the material) for more than about 0.5 nm of contaminants. To minimize the contaminants on internal optical surfaces, the EUVS was manufactured in a clean environment. The few electronic components and wires required to control and read the silicon diodes are at the back of the optical housing and are kept extremely clean. The entire package was stored with a dry nitrogen purge or in a vacuum during most of its testing and prelaunch storage activities. Zeolite absorbers inside the optical housing are designed to capture any residual contaminants that remain inside the optical housing after launch.